An extended irreversible thermodynamic modelling of size-dependent thermal conductivity of spherical nanoparticles dispersed in homogeneous media

G. Lebon[a], **H. Machrafi** [a,*], **M. Grmela** [b]

[a] *Thermodynamics of Irreversible Processes, Liège University, Allée du 6 août, B 4000 Liège, Belgium*

[b] D*epartment of Chemical Engineering, Ecole Polytechnique de Montréal, Montréal, Canada H3C 3A7*

*Corresponding author

E-mail addresses: g.lebon@ulg.ac.be (G. Lebon), h.machrafi@ulg.ac.be (H. Machrafi), miroslav.grmela@polymtl.ca (M. Grmela).

Abstract. The effective thermal conductivity of nanocomposites constituted by nanoparticles and homogeneous host media is discussed from the point of view of Extended Irreversible Thermodynamics. This formalism is particularly well adapted to the description of small length scales. As illustrations, dispersion of *Si* nanoparticles in *Ge* (respectively SiO_2 in epoxy resin) homogeneous matrices are investigated, the nanoparticles are assumed to be spherical with a wide dispersion. Four specific problems are studied: the dependence of the effective thermal conductivity on the volume fraction of particles, the type of phonon scattering at the interface particle-matrix, the radius of the nanoparticles and the temperature.

Keywords: thermal conductivity, nanocomposites, extended thermodynamics, phonon gas

1. Introduction

Nanofluids and nanocomposites have considerably matured during the last decades, both from the fundamental and the applied points of view. They have been used in a wide variety of applications linked to their potential to develop significant modifications of thermal heat transfer properties [1-4]. The change in thermal conductivity has also been exploited to obtain enhancements in the figure of merit Z of thermoelectric materials [5] which behaves as the inverse of the heat conductivity. Many nanostructured materials have overcome the limit $ZT = 1$, for instance ZT=2.4 in Bi_2Te_3 or Sb_2Te_3 [6] and a ZT=2.6 in layered SnSe crystals [7].

In this work, we focus on the discussion on how the presence of nanoparticles fundamentally modifies the effective thermal conductivity of nanocomposites. The subject is of interest as confirmed by the numerous publications during the last decade. The change in the effective heat conductivity is, amongst others, linked to the nature and properties of the host matrix and the nanoparticles, and more particularly to the volume fraction of nanoparticles, their dimension, the nature of particle–matrix interface, the temperature. At the theoretical level, one of the main problems that occur is related to the choice of the analytical expression of the effective heat conductivity of the nanocomposite in terms of the heat conductivities of the matrix and the imbedded particles. The problem can be approached by solving directly the Boltzmann equation for a phonon gas but it raises many difficulties from a mathematical point of view and more particularly with regard to the nature of the boundary conditions. Another option is to use ad hoc analytical expressions, obtained by correlating several data, e.g. [8,9]; the shortcomings of such formulations is their limited applicability and

their lack of physical background. Several works are based on Fourier's heat conduction law, e.g. [10], (see also [9,11] for an overview) which is not applicable when the dimensions of the system are comparable or smaller than the mean free path of the heat carriers [12,13]. Here, our objective is to go beyond Fourier's law and to avoid solving Boltzmann's transport equation. This is achieved by constructing a phenomenological approach axed on one of the latest developments of non-equilibrium thermodynamics, namely Extended Irreversible Thermodynamics [14,15]. This formalism has proved to be particularly well suited to describe systems at short time and small length scales and has been applied in previous work for the description of a transient temperature profile through a nano-film. It is the use of Extended Irreversible Thermodynamics which provides a new and original approach to the problem.

The working hypotheses of the present theoretical study are the following:

- The nanoparticles take the form of rigid homogeneous non-porous spheres.
- The spheres are distributed randomly in the matrix.
- The matrix element is homogeneous.
- Nanoparticles aggregations are not taken into account.
- The material parameters used in the calculations are those of the Debye model [16,17]

One may find in the literature several mathematical expressions of the effective heat conductivity of nanosystems, e.g. [9,11]. In the present work, we will use the following relation that finds its origin in an analogous derivation for the electrical conductivity of rigid particles in a fluid by Maxwell [17], and improved later on by Bruggeman [18]: accordingly, the effective heat conductivity will be given by

$$\lambda_{eff} = \lambda_m \frac{(1+2\alpha)\lambda_p + 2\lambda_m + 2\varphi[(1-\alpha)\lambda_p - \lambda_m]}{(1+2\alpha)\lambda_p + 2\lambda_m - \varphi[(1-\alpha)\lambda_p - \lambda_m]}, \qquad (1.1)$$

where the symbol φ stands for the volume fraction of the dispersed particles, λ_m and λ_p for the heat conductivities of the matrix and the particles respectively, α is a dimensionless parameter accounting for the interactions at the particle-matrix interface [19] and given by

$$\alpha = \frac{R\lambda_m}{r_p}, \qquad (1.2)$$

where r_p is the radius of the spherical particles, R is a measure of the interfacial boundary resistance and $R\lambda_m$ is the so-called Kapitza radius. If $R=0$, whence $\alpha=0$, the interface is called a perfect interface. Relation (1.2) leads to satisfactory predictions in the case of diffuse scattering for which Chen [16] establishes the result

$$R = 4\frac{c_m^v v_m + c_p^v v_p}{c_m^v v_m c_p^v v_p}, \qquad (1.3)$$

with c^v_i and v_i $(i=m, p)$ designating the volumetric specific heats and phonon group velocities respectively.

Our task is to determine the values of the quantities λ_m, λ_p and α that enter in expression (1) of the effective heat conductivity λ_{eff} in terms of the volume fraction, nanoparticles radius, degree of specularity of the interface particle-matrix and temperature. The heat conductivity λ_m as well as the coefficient α will not raise much problems as they will generally be obtained from experimental data and /or well established models; the determination of the quantity λ_p is a source of difficulty because of the small dimensions of the particles and demands a special treatment; it represents the essential motivation of the present analysis based on Extended Irreversible Thermodynamics [14,15]. As shown in the appendix, wherein we briefly recall the ingredients of this formalism, the expression for λ_p is given by

$$\lambda(Kn) = \frac{3\lambda_0}{4\pi^2 Kn^2}\left[\frac{2\pi Kn}{arctg(2\pi Kn)} - 1\right]. \qquad (1.4)$$

where the Knudsen number $Kn = l/r_p$ with l the mean free path of the phonons. It is checked that for $Kn \to \infty$, expression (1.4) tends to 1/Kn indicating a linear dependence with respect to the radius r_p which is the observed asymptotic behavior in nanostructures.

In the first part of Section 2, we study the influence on the effective heat conductivity of the volume fraction of particles concomitantly with their dimension and the nature of the interface between particles and matrix. Two illustrations are considered: uniform dispersion of Si particles in Ge and SiO_2 particles embedded in epoxy resin; the results are compared with other models and experimental data. The second part of Section 2 is devoted to the study of the variations of the effective heat conductivity with the temperature. Final comments and comparison with two other models are found in Section 3.

2. Modelling effective heat conductivity in nanocomposites

Our objective is to determine the dependence of the effective heat conductivity λ_{eff} of nanocomposites on the volume fraction of the nanoparticles, their size, the nature of the interface (either diffusive or specular) and the temperature.

2.1 Volume fraction and size dependence

We first consider the simplified case of a fixed temperature, say *at* room temperature. To determine the volume fraction and size dependencies of $\lambda_{eff,,}$ we need the expressions of the

heat conductivities λ_m and λ_p of the matrix and the particles respectively. Determining λ_m will not raise much problems, indeed it is sufficient to use for it the classical expression

$$\lambda_m = (1/3) c_m^v \, v_m \, l_m , \tag{2.1}$$

referred to by Chen [16,20] as Debye's model, a widely accepted approximation in the literature on nanostructures, e.g. [21-24]; in expression (2.1), the quantity; c_m^v is the volumetric heat capacity, v_m the speed of sound and l_m the mean free path expressed by the empirical Matthiesen rule

$$\frac{1}{l_m} = \frac{1}{l_{m,b}} + \frac{1}{l_{m,coll}} , \tag{2.2}$$

subscripts *b* and *coll* denoting the bulk and collisions contributions respectively. The following relation for the collision mean free path will be used

$$l_{m,coll} = \frac{4 r_p^s}{3\varphi} , \tag{2.3}$$

This expression was proposed and used by Minnich & Chen [19] and Ordonez-Miranda et al. [25]. Note that the maximum volume fraction φ is the one corresponding to the maximum packing of hard spherical particles, i.e. $\varphi_{max} = \pi/\sqrt{18} < 1$.

To take into account the nature of the collisions at the interface matrix-particle, we have, following Dames & Chen [26], replaced the particle radius r_p by the quantity

$$r_p^s = \frac{1+s}{1-s} r_p \quad (0 \le s \le 1), \tag{2.4}$$

the parameter *s* standing for the probability of specular diffusion of the phonons on the particle–matrix interface*; s=0* is characteristic of diffusive collisions while *s=1* denotes pure specular interactions.

Let us now determine the expression of λ_p which will be different from that of λ_m as we must take into account the size dependence of the thermal conductivity. In the following, we will use the result (1.4) provided by EIT and write λ_p in the form

$$\lambda_p = (\frac{1}{3} c_p^v v_p l_{p,b}) \frac{3}{4\pi^2 Kn^2} \left[\frac{2\pi Kn}{arctg(2\pi Kn)} - 1 \right], \tag{2.5}$$

with the Knudsen number defined by $Kn = l_{p,b} / r_p^s$, the terms between parentheses designates the bulk contribution while the remaining terms are related to the size dependence of the heat conductivity of the nanoparticles. Substitution of relations (2.1) and (2.5) – after use has been made of (2.2) and (2.3) – in (1.1) yields the final expression of the effective heat conductivity of the nanocomposite.

The above model will be illustrated by two examples, namely Silicium (Si) particles dispersed in Germanium (Ge), and Silica (SiO_2) particles embedded in an epoxy resin. The latter example has been selected because it allows to compare with experimental data, moreover the effective heat conductivity is seen to increase with the volume fraction instead of decrease as observed for Si-Ge. The system Si-Ge has been the subject of much attention during the last years as attested by the works of Wang & Mingo [27] and Kim et al. [28].

First, calculations have been performed for the couple Si-Ge with three different values for the radius of the Si nanoparticles (r_p = *5, 25, 100 nm*) and for *s=0, 0.2, 1*. The values for these calculations are given in Table 1. The corresponding results are reported in Fig.1, in this figure and in the following ones, the volume fraction is limited to the value $\varphi = \pi/\sqrt{18}$, which corresponds to the maximum packing of hard spherical spheres, as discussed earlier.

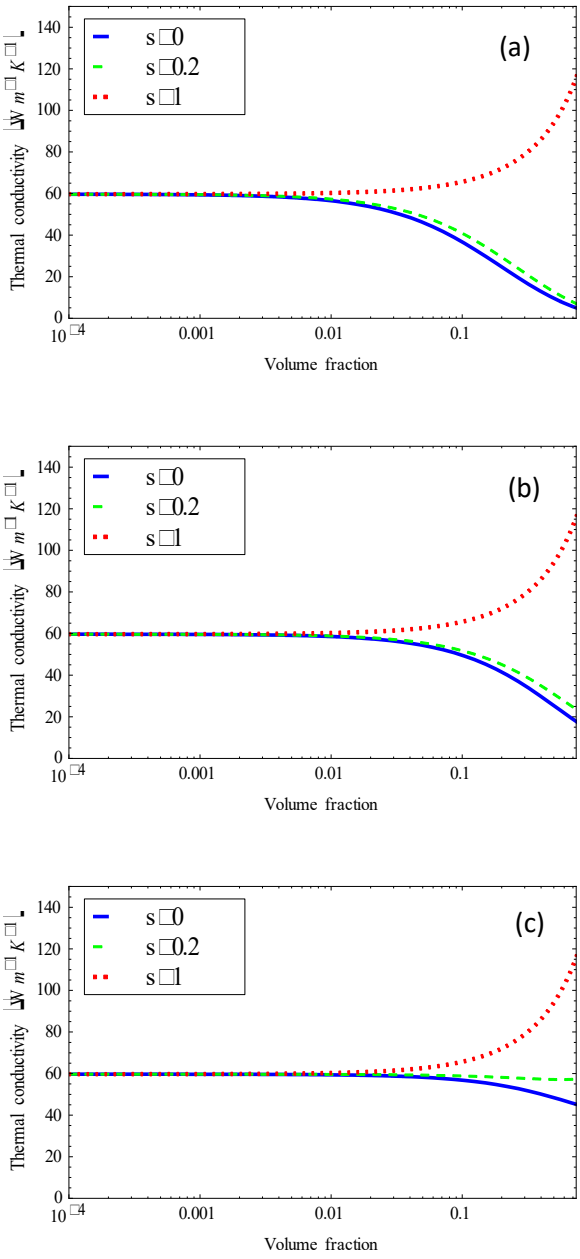

Figure 1. Effective heat conductivity of Si-Ge nanocomposite versus the volume fraction of Si nanoparticle at room temperature for different radii r_p = *5 nm(*a), *25 nm* (b), *100 nm* (c) and different *s* values (*s=0, 0.2, 1*).

Although expression (1.3) of the thermal boundary resistance coefficient R was derived in the diffuse limit [16], we have checked its validity by taking a non-zero s value ($s= 0.2$), and even the extreme case of a pure specular surface $s=1$, by comparing our results with those of [21], who include specular scattering in their developments. We observe good agreement indicating that approximation (1.3) used for R is valid outside its strict range of applicability. Our results agree also with Monte-Carlo simulations as performed by Jeng et al. [29]. Fig. 1 indicates that whatever the values of the radius, λ_{eff} remains practically constant up to values of φ close to 0.01 after which, it gradually decreases. This is true for small s-values but not for $s=1$ for which a steep increase takes place especially at high φ-values. The same behavior was noticed by Behrang et al. [21] but the correspondence is only qualitative because it must be kept in mind that the applicability of our model is restricted to small s-values. It should also be noticed that our numerical values are slightly larger than those of Behrang et al. [21] and Minnich & Chen [19], principally for large radii (around 100 nm). This is not surprising as these authors utilize different values for the material parameters, based on the dispersion rather than on Debye's model. When we repeat our calculations with the dispersion approximation, the differences between our description and those of Minnich-Chen and Behrang et al. become minute.

It may seem strange that the thermal conductivity of the composite Si-Ge is smaller than that of the pure matrix Ge when the volume fraction of particles in increased. Indeed, since bulk Si has a larger thermal conductivity than bulk Ge, one should expect that composite conductivity will be higher. The reduction of the conductivity finds its interpretation in the small dimensions of the particles. Indeed, relation (1.4) tells us that the thermal conductivity of nanospheres of radii comparable or smaller than the mean free path of heat carriers may be

considerably less than that of the bulk, hence a decrease of the effective heat conductivity of the composite. Moreover, the smaller is the radius, the smaller the thermal conductivity of the nanoparticles. Similar results are also observed in Si_xGe_{1-x} alloys [27].

A further check of the validity of the model is provided by calculating the effective heat conductivity of a different material, namely SiO_2 particles embedded in epoxy resin for which experimental data are available [30]. As shown in Fig.2a, the effective heat conductivity λ_{eff} is slightly growing linearly with particle volume fraction φ up to φ =0.1 followed by a steep increase, A zoom of the results in the region $0<\varphi<0.1$ (see Fig. 2b) exhibits the quasi-linear growth of λ_{eff} and the good accord with the experimental data. In contrast with Si-Ge, the effective heat conductivity of the SiO_2-epoxy composite is increasing with the nanoparticle density. Our analysis indicates that the boundary properties and the particles dimension play a decisive role in the decrease or increase of thermal conductivity. A possible interpretation of the observed behaviors may be found in the value of the dimensionless α ($=R\lambda_m/r_p$) parameter which is much smaller in the case of SiO_2-epoxy than for Si-Ge of the order 50 to 200 depending on the values of r_p and s. For $\alpha>1$, λ_{efff} is decreasing while for $\alpha<1$, λ_{eff} is increasing. This result reflects the relative importance of the dimension r_p of the particles with respect to the Kapitza radius $R\lambda_m$. For a given value of the thermal resistance R, the less is the radius of the particles, the less is the thermal conductivity as clearly exhibited by Figs. 1-3 and 4. The value of the α-parameter is of importance within the perspective of practical applications: constituents with small α-values should be selected when significant enhancement of the thermal conductivity is aimed at while large values should be preferred when a reduction of phonon transport is the objective.

In Table 1 are listed the material parameters [16] used in the calculations.

Table 1. Material parameters (at room temperature)

Material	Model	Specific heat x 10^6 J/m³K	Mean free path l_b nm	Group velocity m/s
Si		1.66	40.9	6400
Ge		1.67	27.5	3900
SiO_2		1.687	0.558	4400
Epoxy		1.91	0.11	2400

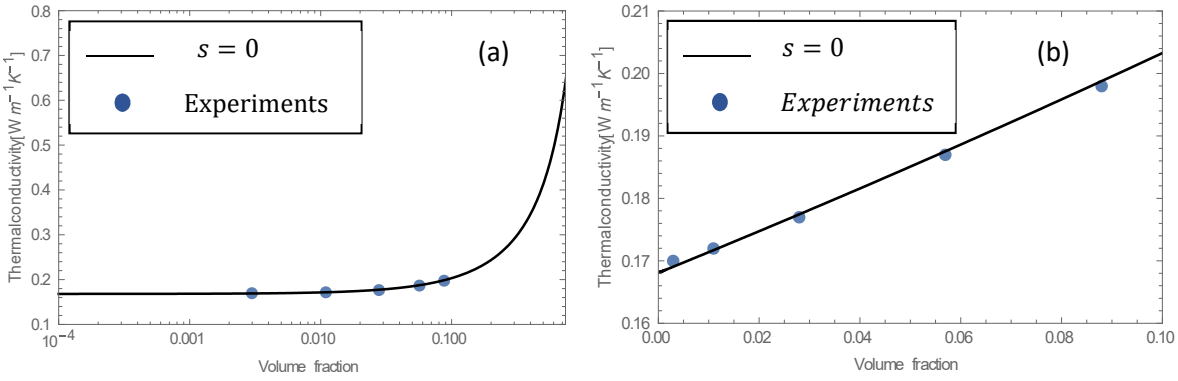

Figure 2. Effective heat conductivity of SiO_2 embedded in an epoxy resin versus the volume fraction and comparison with experimental data at room temperature (r_p=10 nm, s=0). General trend in the region 0<φ<1 (a). Zoom on the region 0< φ <0.10 (b).

2.2. *Temperature dependence*

The temperature dependence of the heat conductivity will appear implicitly through the frequency ω dependence of the various quantities appearing in the general expression

$$\lambda = \frac{1}{3}\int_0^{\omega_D} c_v(T,\omega)v(T,\omega)l(T,\omega)d\omega. \qquad (2.6)$$

The determination of λ_{eff} as given by relation (1.1) requires therefore the knowledge of $c_j^v(T,\omega), v_j(T,\omega), l_{j,b}(T,\omega)$ for j = *m, p* and $l_{m,\,coll}(T)$ in terms of ω and T, note that in the expression of the particle mean free path, only the bulk free path is needed. The limit of integration, ω_D, is the Debye frequency cutoff: ω_D = 5.14 10^{-13} s^{-1} for Ge and 9.12 10^{-13} s^{-1} for Si. In agreement with [31-33], we assume that the group velocity v is independent on T and ω while the heat capacity and the bulk mean free path are given respectively by

$$c_j^v = \frac{3\hbar^2}{2\pi^2 v_j^3 k_B T^2}\frac{\omega^4 \exp(\hbar\omega/k_B T)}{[\exp(\hbar\omega/k_B T)-1]^2}, \quad j= m, p \qquad (2.7)$$

$$\frac{1}{l_{j,b}} = B_j T\omega^2 \exp(-\frac{\theta_j}{T}), \quad j= m, p \qquad (2.8)$$

wherein B_j and θ_j are constant quantities obtained by fitting experimental data measured by Glassbrenner & Slack [34]. We are now in possession of all the elements needed to evaluate the effective heat conductivity of the nanocomposite as expressed by relation (1.1). To be explicit, the heat conductivity λ_m of the matrix element is directly derived from (2.6) with the mean free path in the matrix $l_m(T, \omega)$ given by $1/l_m(T,\omega) = 1/l_{m,b}(T,\omega) + 3\varphi/4r_p^s$ (see relations (2.2) and (2.3)) while, accordingly to (2.5), λ_p will be written as

$$\lambda_p = \frac{1}{4\pi^2}\int_0^{\omega_D} c_p^v(T,w)v_p l_{p,b}(T,\omega)\frac{1}{Kn(T,\omega)^2}\left\{\frac{2\pi Kn(T,\omega)}{arctg[2\pi Kn(T,\omega)]}-1\right\}d\omega, \qquad (2.9)$$

with $Kn = l_{p,b}/ r_p^s$. The results for the effective heat conductivity λ_{eff} of the composite Si-Ge are reported in Figs. 3(a) through 3(c) as a function of the volume fraction φ of Si particles, temperature T and the specularity coefficient s. It is shown that λ_{eff} decreases with the temperature whatever the radius of the nanoparticles and the s coefficient; at high temperature ($T= 500\ K$) and large r_p-values (around 100 nm), the heat conductivity remains practically constant. By comparing the curves for $s=0$ and $s=0.2,$ one observes no drastic changes. A more detectable modification is observed for $s=0.5$ and especially for $a_p = 100\ nm$ for which an increase of λ_{eff} is observable at φ-values of larger than 0.5.

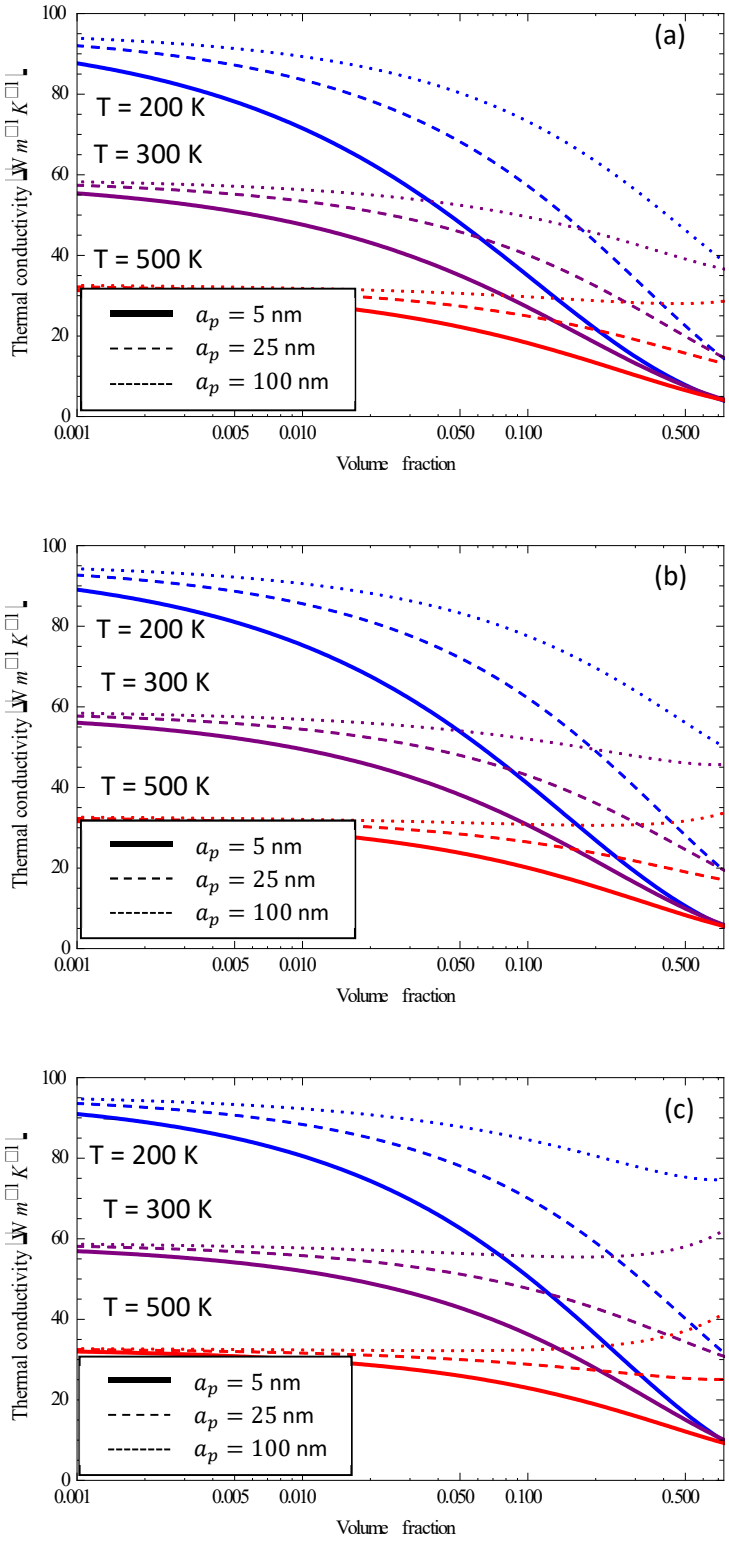

Figure 3. Effective heat conductivity of Si-Ge nanocomposite versus the volume fraction at three different temperature: *T=200K* (upper curves), *T= 300K* (middle curves), *T= 500K*

(bottom curves), different radii r_p = *5*, *25*, *100 nm* and different *s* values *s=0* (a), *s= 0.2* (b), *s=0.5* (c).

We have represented on Figs. 4(a-c) the effective heat conductivity versus the temperature for three values of the volume fraction φ*= 0.01, 0.2* and *0.5, s* being fixed equal to zero while the values o*f* r_p are the same as previously, namely r_p *= 5, 25, 100 nm.*

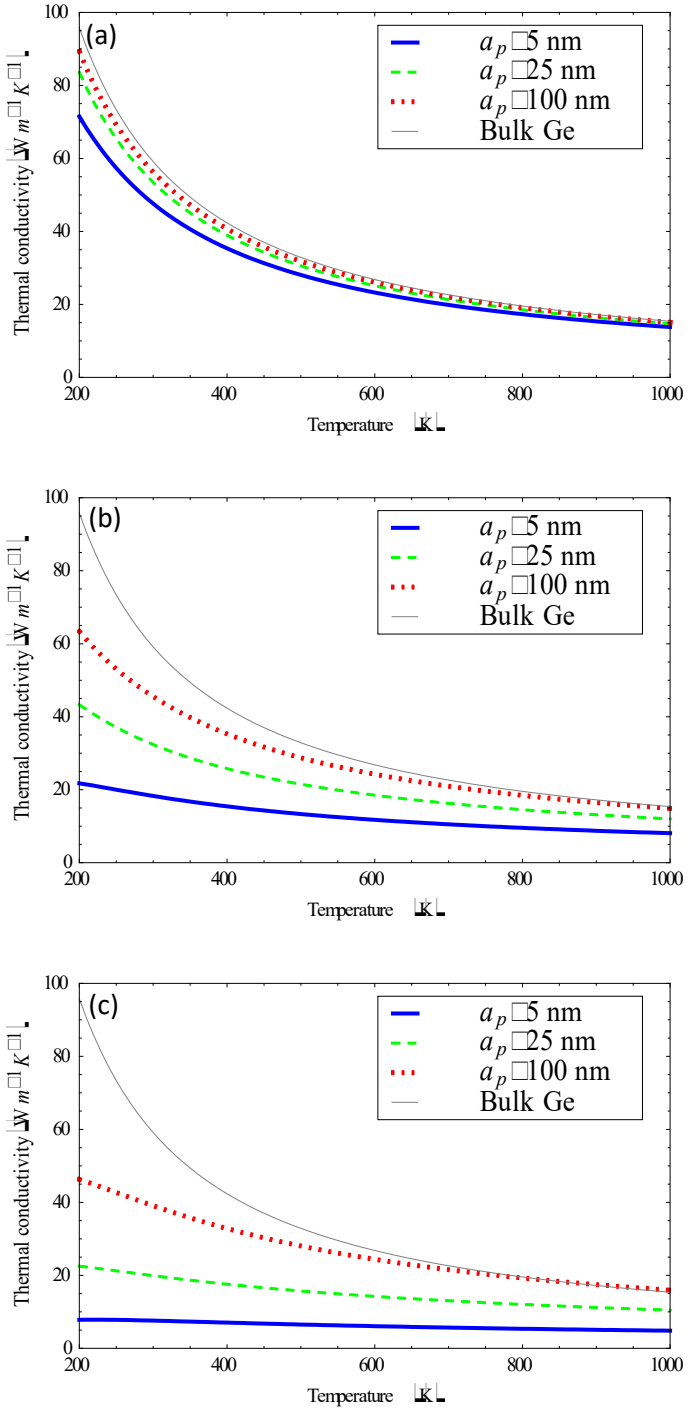

Figure 4. Effective thermal conductivity of Si-Ge versus the temperature at three different values of the volume fraction: $\varphi=0.01$(a), $\varphi=0.2$(b), $\varphi=0.5$(c) for $r_p=5,\ 25,\ 100\ nm$, with s = 0. For the sake of comparison, the values λ_m for pure Ge are also plotted.

To emphasize the role of the presence of nanoparticles on the composite heat conductivity, we have drawn the curve corresponding to a pure Ge crystal; the reduction of λ_{eff} becomes more important as the size of the particles becomes small and the volume fraction large. The decrease of λ_{eff} with temperature may be explained as follows: by increasing the temperature, one causes an increase of the thermal resistance whence a diminution of thermal conductivity. This effect is less pronounced for smaller radii of the particles, because of the increase of the particle matrix interface. This can be interpreted by saying that phonons will meet more obstacles with, as a consequence, a reduction of heat transport. Heat conductivity is practically insensitive to temperature variations at high volume fractions ($\varphi>0.5$) and small nanoparticles ($r_p < 5nm$). Our results are qualitatively similar to those obtained by Behrang et al. (2013) with the differences that they restrict themselves to diffusive scattering ($s=0$) with nanoparticles radii from 10 to 50 nm versus 5 to 100 nm in the present paper

3. Final comments

Our objective is to study the change in heat conductivity resulting from the dispersion of spherical nanoparticles in homogeneous host media in the framework of Extended Irreversible Thermodynamics [11,14,15], whose basic concepts are recalled in the appendix. The dependence with respect to several factors as volume fraction, particles radius, nature of the interface and temperature is examined. The originality of the present model is the derivation of the expression of the heat conductivity of the nanoparticles.

The most important result of the present paper is embedded in equation (2.5). It makes explicit the dependence of the heat conductivity of the nanoparticles on their size through the

Knudsen number l_p / r_p^s, the type of phonon-interface scattering (either diffusive or specular) and temperature. All the results are easily exploitable and reproducible as they are given by mathematical analytical expressions directly tractable with Mathematica.

The model predicts numerical values which are of the same order of magnitude as those obtained by other authors as Minnich & Chen [19] and Behrang et al. [21] whose predictions match Monte-Carlo simulations. The observation that our results are in good agreement with other ones based on different models attests of the validity of the present approach.

The results plotted in Fig. 1 indicate that the effective heat conductivity λ_{eff} of Si-Ge composite is decreasing with the nanoparticles density and that at a fixed volume fraction, λ_{eff} is decreasing with decreasing radii. Such an effect may be of interest within the perspective of an optimal conversion of heat transport into electric current; indeed, the efficiency of this conversion is measured by means of the so-called figure of merit defined by $Z = \sigma_e \varepsilon^2 / \lambda$, with σ_e the electrical conductivity and ε the Seebeck coefficient so that a lowering of the heat conductivity λ will clearly contribute to a better efficiency.

Most works are silent about variation of the effective heat conductivity λ_{eff} with the temperature. This subject is discussed in the second part of Section 3, where it is shown that increasing the temperature results in a decrease of the effective thermal conductivity, in particular, the variations of λ_{eff} with temperature are seen to be less important for small radii and large volume fractions.

Although our work compares well with that of Behrang et al. [21], it is important to underline their differences. First, Behrang et al. analysis is not based on non-equilibrium thermodynamics but follows a hybrid route mixing EMA approach and Boltmann's theory; in

particular, they center all their developments on the notion of probability of phonon transmission from particles to matrix, not used in our approach. To examine the role of volume fraction, Behrang et al. make use of the dispersion model [16,20], but they replace it by Debye's one to examine the temperature effects. Here, for the sake of homogeneity, Debye's model is used throughout the whole work. This is also the reason why we use different values for the material parameters. Another important difference is that Behrang et al. assume everywhere that the non-dimensional parameter α is zero meaning that they do not take into account the Kapitza resistance between nanoparticles and matrix. To account for specular diffusion, we simply redefine the particulate radius (see relation (2.4)) as proposed by Dames & Chen [26], instead, Behrang et al., calculate separately the contributions $\lambda_{eff}^{(s)}$ and $\lambda_{eff}^{(d)}$ from the specular and diffusive effects respectively and write the heat conductivity of the effective medium as the arithmetic average $\lambda_{eff} = s\lambda_{eff}^{(s)} + (1-s)\lambda_{eff}^{(d)}$.

It is our purpose to extend our analysis to non-spherical nanoparticles, say ellipsoidal or cylindrical shapes such as carbon nanotubes and explore important effects like particle agglomeration and the role of porosity which were not dealt with in the present approach. Extensions to include spatially ordered distributions, such as superlattices [35] and graded materials, will also be the subject of future investigations.

Data accessibility

This work contains no experimental data. To obtain further information on the models underlying this paper please contact h.machrafi@ulg.ac.be.

Competing interests

We declare we have no competing interests.

Authors' contributions

G.L. performed the theoretical developments with contributions from H.M. The paper was written by G.L. with contributions from H.M and M.G. H.M. performed the calculations. All authors gave final approval for publication.

Acknowledgements

The authors wish to thank drs. A. Behrang (Ecole Polytechnique de Montréal) and A. Sellitto (University Basilicata, Italy) for providing useful data about the nanomaterials investigated in the present work. One of us (G.L) is indebted to the Wallonie-Bruxelles-Quebec 9th CMP (biennium 2015-2017) for giving him the opportunity to visit our colleagues of the department of Chemical Engineering at Ecole Polytechnique de Montreal.

Funding statement

The work of H.M. is funded by BelSPo.

Appendix: A brief review of Extended Irreversible Thermodynamics

The description of systems at subscales, as nanoparticles and high–frequency processes, requires to go beyond the classical theory of irreversible processes as proposed some decades ago by Onsager [36,37] and Prigogine [38] amongst others. Indeed this formalism is based on the local equilibrium hypothesis which limits its range of application to large time and space scales. More recently, some authors have proposed an alternative approach, referred to as Extended Irreversible Thermodynamics (EIT), covering a wider class of processes and systems. The principal idea behind EIT is to elevate the dissipative fluxes, as the fluxes of mass, energy and momentum to the status of independent variables at the same level as the classical variable like mass, energy or momentum. As a consequence, the space $\boldsymbol{V}$ of state variables will be formed by the union of the (slow and conserved) classical variables $\boldsymbol{C}$ and the (fast and non-conserved) flux variables $\boldsymbol{F}$ so that $\boldsymbol{V}= \boldsymbol{(C \, U \, F)}$.

As a case-study, let us consider heat conduction in a rigid body at rest, the generalization to more complicated systems as fluids, mixtures, suspensions, polymer solutions, porous media and others have been dealt with in detail in numerous publications and books, e.g. [11,14,15,39]. In the problem of a rigid heat conductor, the only relevant conserved variable is the internal energy e (or the temperature T) whereas the energy flux (here the heat flux vector $\boldsymbol{q}$) is the non-conserved flux variable so that the space of state variables is $\boldsymbol{V}= \boldsymbol{(e, q)}$. In more complex materials like in nanomaterials, fluxes of higher order should be introduced as shown later on. The corner stone of EIT is to assume the existence of an entropy function $\eta(\boldsymbol{V})$, depending on the whole set $\boldsymbol{V}$ of variables: here $\eta= \eta(e \, ,\boldsymbol{q})$, or in terms of time derivatives,

$$d_t\eta = \frac{\partial \eta}{\partial e} d_t e + \frac{\partial \eta}{\partial \boldsymbol{q}} . d_t \boldsymbol{q} \,, \tag{A.1}$$

wherein e and η are measured per unit volume and a dot stands for the scalar product. The symbol d_t designates the time derivative which is indifferently the material or the partial time derivative as the system is, respectively, in motion or at rest. It is assumed that s is a concave function of the variables to guarantee stability of the equilibrium state and that it obeys a general time-evolution equation of the form

$$d_t\eta = -\nabla . \boldsymbol{J}^s + \sigma^s \qquad (\sigma^s \geq 0) \,, \tag{A.2}$$

whose rate of production per unit volume σ^s (in short, the entropy production) is positive definite to satisfy the second principle of thermodynamics, the quantity $\boldsymbol{J}^s$ is the entropy flux. Let us define the local non-equilibrium temperature by $T^{-1}(e) = \partial \eta / \partial e$ and select the constitutive equation for $\partial \eta / \partial \boldsymbol{q}$ as given by $\partial \eta / \partial \boldsymbol{q} = -\gamma(T)\boldsymbol{q}$, where $\gamma(T)$ is a material coefficient depending generally on T; it is positive definite in order to meet the property that s is maximum at equilibrium, the minus sign in front of $\gamma(T)\boldsymbol{q}$ has been introduced for convenience. Under these conditions, expression (A.1), referred to as the Gibbs equation, can be written as

$$d_t\eta(e, \boldsymbol{q}) = T^{-1} d_t e - \gamma \boldsymbol{q} . d_t \boldsymbol{q} \tag{A.3}$$

Eliminating $d_t e$ by means of the energy balance which, in absence of heat sources, can be written as

$$d_t e = -\nabla . \boldsymbol{q} \,, \tag{A.4}$$

yields

$$d_t\eta = -\nabla\frac{\boldsymbol{q}}{T} + \boldsymbol{q}.(\nabla T^{-1} - \gamma d_t\boldsymbol{q}) \quad . \qquad \text{(A.5)}$$

From the comparison with the general balance relation (A.2) follows the identification

$$\boldsymbol{J^s}=\boldsymbol{q}/T \text{ (entropy flux)}, \quad \sigma^s = \boldsymbol{q}.(\nabla T^{-1} - \gamma d_t\boldsymbol{q}) \geq 0 \text{ (entropy production)}. \qquad \text{(A.6)}$$

The expression for σ^s is a bilinear relationship in the flux $\boldsymbol{q}$ and the quantity represented by the two terms between the parentheses that is usually called the thermodynamic force $\boldsymbol{X}$. The simplest way to guarantee the positiveness of the entropy production σ^s is to assume a linear flux-force relation of the form $\boldsymbol{q}=L\boldsymbol{X}$ *w*here L is a phenomenological coefficient**,** this procedure leads to Cattaneo's law [40]

$$\tau d_t\boldsymbol{q} = -\boldsymbol{q} - \lambda\nabla T\,, \qquad \text{(A.7)}$$

after one has put $\gamma L=\tau$ (relaxation time) and $L/T^2=\lambda$ (heat conductivity) and wherein τ and λ are proven to be positive quantities [14,15]. Although Cattaneo's relation is useful at short time scales (high frequencies), it is not satisfactory with the purpose to describe heat transport at short length scales wherein non-localities play a preponderant role.

Non-local effects are elegantly introduced in the framework of EIT by appealing to a hierarchy of fluxes $\boldsymbol{Q}^{(1)}$, $\boldsymbol{Q}^{(2)}$, ... $\boldsymbol{Q}^{(N)}$ with $\boldsymbol{Q}^{(1)}$ identified with the heat flux vector $\boldsymbol{q}$, $\boldsymbol{Q}^{(2)}$ (a tensor of rank two) as the flux of the heat flux, $\boldsymbol{Q}^{(3)}$ as the flux of $\boldsymbol{Q}^{(2)}$, etc. From the kinetic theory point of view, $\boldsymbol{Q}^{(2)}$, $\boldsymbol{Q}^{(3)}$, ... $\boldsymbol{Q}^{(N)}$ represent the higher moments of the velocity distribution. Written in Cartesian coordinates and designating by f the distribution function, the fluxes are given by

,

$$Q_i^{(1)} \equiv q_i = \int fC^2 C_i d\boldsymbol{c},\ Q_{ij}^{(2)} = \int f\ C^2 C_i C_j d\boldsymbol{c},\ Q_{ijk}^{(3)} = \int f\ C^2 C_i C_j C_k d\boldsymbol{c}, \ldots$$

with $\boldsymbol{C}=\boldsymbol{c}-\boldsymbol{v_m}$ the relative velocity of phonons with respect to their mean velocity $\boldsymbol{v_m}$. Up to the n^{th}-order moment, the Gibbs equation generalizing expression (A.3) takes the form

$$d_t\eta\left(e, \boldsymbol{q}, \boldsymbol{Q}^{(1)}, \ldots, \boldsymbol{Q}^{(N)}\right) = T^{-1} d_t e - \gamma_1 \boldsymbol{q} \cdot d_t \boldsymbol{q} - \gamma_2 \boldsymbol{Q}^{(2)} \otimes d_t \boldsymbol{Q}^{(2)} - \cdots - \gamma_N \boldsymbol{Q}^{(N)} \otimes d_t \boldsymbol{Q}^{(N)}, \tag{A.8}$$

while instead of (A.6a) the entropy flux reads as

$$\boldsymbol{J}^s = T^{-1}\boldsymbol{q} + \beta_1 \boldsymbol{Q}^{(2)}.\boldsymbol{q} + \ldots \beta_{N-1} \boldsymbol{Q}^{(N)} \otimes \boldsymbol{Q}^{(N-1)}, \tag{A.9}$$

the symbol $\otimes$ denotes the inner product of the corresponding tensors. For instance, in Cartesian coordinates and using the summation convention on repeated indices, $\boldsymbol{Q}^{(3)} \otimes \boldsymbol{Q}^{(2)}$ stands for $Q_{ijk} Q_{jk}$. We have limited ourselves to the simplest form of the entropy and the entropy flux which are sufficient for the present purpose. The entropy production σ^s which in virtue of (A.2), is given by

$$\sigma^s = d_t \eta + \nabla . \boldsymbol{J}^s, \tag{A.10}$$

is easily derived by substituting $d_t\,\eta$ and $\boldsymbol{J}^s$ from (A.8) and (A.9) respectively and by eliminating $d_t\, e$ via the energy balance (A.4), the result is

$$\sigma^s = -(-\nabla T^{-1} + \gamma_1 d_t \boldsymbol{q} - \beta_1 \nabla . \boldsymbol{Q}^{(2)}).\boldsymbol{q} \ldots - \sum_{n=2}^{N} \boldsymbol{Q}^{(n)} \otimes (\gamma_n d_t \boldsymbol{Q}^{(n)} - \beta_n \nabla . \boldsymbol{Q}^{(n+1)} - \beta_{n-1} \nabla Q^{(n-1)}) \geq 0 \tag{A.11}$$

The above bilinear expression in fluxes and forces (the quantities between parentheses) suggests the following hierarchy of linear flux-force relations

$$\nabla T^{-1} - \gamma_1 d_t \boldsymbol{q} + \beta_1 \nabla \cdot \boldsymbol{Q}^{(2)} = \mu_1 \boldsymbol{q}\,, \tag{A.12}$$

$$\beta_{n-1} \nabla \boldsymbol{Q}^{(n-1)} - \gamma_n d_t \boldsymbol{Q}^{(n)} + \beta_n \nabla \cdot \boldsymbol{Q}^{(n+1)} = \mu_n \boldsymbol{Q}^{(n)}\,,\ (n=2,3\ldots N.)\,, \tag{A.13}$$

the latter can also be viewed as time evolution equations for the fluxes $\boldsymbol{q}, \boldsymbol{Q}^{(2)} \ldots\ Q^{(N)}$. Making use of (A.12) and (A.13), expression (A.11) of the entropy production becomes

$$\sigma^s = \mu_1 \boldsymbol{q}.\boldsymbol{q} + \mu_2 \boldsymbol{Q}^{(2)} \otimes \boldsymbol{Q}^{(2)} + \ldots \mu_N \boldsymbol{Q}^{(N)} \otimes \boldsymbol{Q}^{(N)} \geq 0\,, \tag{A.14}$$

with $\mu_n \geq 0$ (n= *1,2, ...n)*to satisfy the positiveness of the entropy production.

To gain insight about the physical meaning of the various phenomenological coefficients, let us assume absence of non-locality so that the term in $\nabla.\boldsymbol{Q}^{(2)}$ will not appear in (A.12) which reduces to Cattaneo's relation. If in addition, one considers steady situations, the term in $d_t\boldsymbol{q}$ vanishes and one recovers Fourier's law. These observations lead to the following identities

$$\mu_1 = 1/\lambda T^2, \gamma_1 = \tau/\lambda T^2\,, \tag{A.15}$$

indicating that μ_1 is related to the heat conductivity λ and γ_1 to the relaxation time τ. The identification of the higher order coefficients is not so easy as its demands to compare with higher order evolution equations, but it is expected that the parameters μ_n and γ_n are related to coefficients of thermal conductivity λ_n and relaxation times τ_n of order n respectively. Moreover, since $\boldsymbol{Q}^{(n+1)}$ is the flux of $\boldsymbol{Q}^{(n)}$, this implies, by the very definition of a flux, that $d_t\boldsymbol{Q}^{(n)} = -\nabla.\boldsymbol{Q}^{(n+1)}$; now, when dividing (A.12) by γ_1 and (A.13) by γ_n *(n=2,3,...)*, it follows that $\beta_1/\gamma_1 = -1, \beta_2/\gamma_2 = -1, \ldots$ or, more generally, $\gamma_n = -\beta_n$, which reduces considerably the

number of undetermined coefficients.

We consider now an infinite number of flux variables and apply the spatial Fourier transform $\hat{\boldsymbol{q}}(\boldsymbol{k},t)=\int_{-\infty}^{+\infty}\boldsymbol{q}(\boldsymbol{r},t)e^{-i\boldsymbol{k}.\boldsymbol{r}}d\boldsymbol{r}$ to relations (A.12) and (A.13), with $\boldsymbol{k}$ the wave-number vector and $\boldsymbol{r}$ the position vector; this operation leads to the following time-evolution equation of the Fourier transformed heat flux:

$$\tau d_t\,\hat{\boldsymbol{q}}(\boldsymbol{k})+\hat{\boldsymbol{q}}(\boldsymbol{k})=-i\boldsymbol{k}\lambda(\boldsymbol{k})\hat{T}(\boldsymbol{k}) \tag{A.16}$$

wherein $\tau\equiv\tau_1=\gamma_1/\mu_1$ designates the relaxation time depending generally on $\boldsymbol{k}$ and $\lambda(\boldsymbol{k})$ the continued-fraction for the $\boldsymbol{k}$-dependent effective thermal conductivity:

$$\lambda\,(\boldsymbol{k})=\cfrac{\lambda_0}{1+\cfrac{k^2l_1^2}{1+\cfrac{k^2l_2^2}{1+\cfrac{k^2l_3^2}{1+\ldots}}}}, \tag{A.17}$$

λ_0 is the bulk thermal conductivity independent of the dimension of the system and l_n the mean free path of order n given by

$$l_n^2=\gamma_n^2/\mu_n\mu_{n+1}\,. \tag{A.18}$$

By establishing (A.17), it was assumed that the relaxation times τ_n $(n>1)$ corresponding to the higher order fluxes are negligible with respect to τ which is a hypothesis generally well admitted in kinetic theories. We now select the mean free path l_n of order n in terms of n as - $l^2_n = l^2\,(n+1)^2/\,(4(n+1)^2-1)$, and l identified as the mean free path independent of the order of approximation, this is a natural choice in phonon's kinetic theory as shown by Dreyer &

Struchtrup [41]. Under the above conditions, it was shown by Hess [42] that, in the asymptotic limit ($n\rightarrow\infty$), the continued fraction (A.17) reduces, to

$$\lambda(k)=\frac{3\lambda_0}{k^2l^2}\left[\frac{lk}{arctg(lk)}-1\right]. \qquad \text{(A.19)}$$

In the present problem limited to spherical configurations, there is one single characteristic length r so that it is rather natural to identify the wave number k as $k=2\pi/r$, expressing (A.19) in terms of the Knudsen number $Kn=l/r$, one obtains [43] the relation given by (1.4), namely

$$\lambda(Kn)=\frac{3\lambda_0}{4\pi^2Kn^2}\left[\frac{2\pi Kn}{arctg(2\pi Kn)}-1\right]. \qquad \text{(A.20)}$$

References

1. S.U.S. Choi, J.A. Eastman, *Enhancing Thermal conductivity of Fluids with Nanoparticles*, Argonne Press, Illinois, 1995.

2. C. De Tomas, A. Cantarero, A. F. Lopeandia, F. X. Alvarez, Thermal conductivity of group-IV semiconductors from a kinetic-collective model, *Proc. R. Soc. A*, 470 (2014) 2169.

3. S. Kakak, A. Pramuanjaroenkij, Review of heat transfer enhancement with nanofluids, *Int. J. Heat Mass Transfer* 52 (2009) 3187-3169.

4. W. Tesfai, P.K. Singh, S. Masharga, T. Souier, M. Chiesa, Y. Shatilla Investigating the effects of suspensions nano-structure on the thermophysical properties of nanofluids, *J. Appl. Phys.* 112 (2012) 114315-15.

5. A. Sellitto, V.A. Cimmelli, D. Jou, Thermoelectric effects and size dependency of the figure of merit in cylindrical nanowires, *Int. J. Mass Heat Transfer* 57 (2013) 109-116.

6. R. Venkatasubramanian, E. Siivola, T. Colpitts, B. O'Quinnet, Thin-film thermoelectric devices with high room-temperature figures of merit, *Nature* 413 (2001) 597-602.

7. L.-D. Zhao, S.-H. Lo, Y. Zhang, H. Sun, G. Tan, C. Uher, C. Wolverton, V. P. Dravid, M. G. Kanatzidis, Ultralow thermal conductivity and high thermoelectric figure of merit in SnSe crystals, *Nature* 508 (2014) 373-377.

8. K. Khanafer, K.A. Vafai, A critical synthesis of thermophysical characteristics of nanaofluids *Int. J. Heat and Mass Transfer* 54 (2011) 4410-4428.

9. E.E. Michaelidis, Transport properties of nanofluids. A critical review, *J. Non-Equilib. Thermodyn*. 38 (2013)1-31.

10. C. W. Nan, R. Birringer, D. R. Clarke, H. Gleiter, Effective thermal heat conductivity of particulate composites with interfacial thermal resistance, *J. Appl. Phys.* 81 (1997) 6692-6699.

11. G. Lebon, Heat conduction at micro and nanoscales; A review through the prism of Extended Irreversible Thermodynamics, *J. Non-Equilib. Thermodyn.* 39 (2014) 35-58.

12. V. A. Cimmelli, A. Sellitto, D. Jou, A nonlinear thermodynamic model for a breakdown of the Onsager symmetry and the efficiency of thermoelectric conversion in nanowires, *Proc. R. Soc. A*. 470 (2014) 2170.

13. G. Lebon, H. Machrafi, M. Grmela, Ch. Dubois, An extended thermodynamic model of transient heat conduction at sub-continuum scales, *Proc. R. Soc. A* 467 (2009) 3241-3256.

14. G. Lebon, D. Jou, J. Casas-Vazquez, *Understanding Non-Equilibrium Thermodynamics*, Springer, Berlin, 2008.

15. D. Jou, J. Casas-Vazquez, G. Lebon, *Extended Irreversible Thermodynamics*, 4rth edition, Springer, New York, Dordrecht, Heidelberg, London, 2010.

16. G. Chen, Thermal conductivity and ballistic-phonon transport in the cross-plane direction of superlattices, *Phys. Rev. B* 57 (1998) 14958 -14973.

17. J.C. Maxwell, *Treatise on Electricity and Magnetism*, 2nd edition, Clarendon, Oxford: 1881.

18. D. Bruggeman, Berechnung verschiedener physikalischer Konstanten von heterogenen Substanzen, *Anal. Phys*. 24 (1935) 636-664.

19. A. J. Minnich, G. Chen, Modified effective medium formulation for the thermal conductivity of nanocomposites, *Appl. Phys. Lett.* 91, (2007) 073105-7.

20. G. Chen, Phonon heat conduction in nanostructures*, Int. J. Therm. Sci.* 39 (2000) 471-480

21. A. Behrang, M. Grmela, C. Dubois, S. Turenne, P. G. Lafleur, Influence of particle-matrix interface, temperature and agglomeration of heat conduction in dispersions, *J. Appl. Phys*.114 (2013) 014305.

22. F. Vazquez, J.A. del Rio, Thermodynamic characterization of the diffusive transport to wave propagation transition in heat conducting thin films, *J. Appl. Phys.* 112 (2012) 123707.

23. C. Dames, *Microscale conduction in Heat Conduction*, pp 347-401 (M. Latif, editor), Springer, 2009.

24. A. Sellitto, F.X. Alvarez, D. Jou, Temperature dependence of boundary conditions in phonon hydrodynamics of smooth and rough nanowires, *J. Appl. Phys.* 107 (2010) 114312.

25. J. Ordonez-Miranda, R. Yang, J.J. Alvarado-Gil, On the thermal conductivity of particulate composites, *Appl. Phys. Lett.* 98 (2011) 233111-3.

26. C. Dames, G. Chen, Theoretical phonon thermal conductivity of Si/Ge superlattice nanowires, *J. Appl. Phys.* 95 (2004) 682-693.

27. Z. Wang, N. Mingo, Diameter dependence of SiGe nanowire thermal conductivity, *Appl. Phys. Lett.,* 97 (2010) 101903.

28. H. Kim, I. Kim, H. Choi, W. Kim, Thermal conductivities of Si1-xGex nanowires with different germanium concentrations and diameters, *Appl. Phys. Lett.* 96 (2010) 233106.

29. M. S. Jeng, D. Song, G. Chen, R. Yang, Modeling the thermal conductivity and phonon transport in nanoparticle composites using Monte Carlo simulation, *J. Heat Transfer* 130 (2008) 042410-11.

30. R. Kochetov, A.V. Korobko, T. Andritsch, P. H. F. Morshuis, S. J. Picken, J.J. Smit, Modeling of the thermal conductivity in polymer nanocomposites and the impact of the interface between filter and matrix, *J. Phys. D* 44 (2011) 395-401.

31. J. Callaway, Model for lattice thermal conductivity at low temperature, *Phys. Rev.* 113 (1959) 1046-1051.

32. N. Mingo, L. Yang, D. Li, A. Majumdar, Predicting the thermal conductivity of si and Ge nanowires, *Nano Lett.* 3 (2003) 1713-1716.

33. G. Chen, Nanoscale *Energy Transport and Conversion: A Parallel Treatment of Electrons, Molecules, Phonons, and Photons*, Oxford University Press, Oxford, 2005.

34. C.J. Glassbrenner, G.A. Slack, Thermal conductivity of silicon and germanium from 3°K melting point, *Phys. Rev. A* 134 (1964) 1058-1069.

35. F. X. Alvarez, J. Alvarez-Quintana, D. Jou, J. Rodríguez Viejo, Analytical expression for thermal conductivity of superlattices, *J. Appl. Phys.* 107 (2010) 084303.

36. L. Onsager, Reciprocal relations in irreversible processes I, *Phys. Rev.* 37 (1931) 405-426.

37. L. Onsager, Reciprocal relations in irreversible processes II, *Phys. Rev.* 38 (1931) 2265-2279.

38. I. Prigogine, *Introduction to Thermodynamics of Irreversible Processes*, Interscience, New York, 1961.

39. D. Jou, J. Casas-Vazquez, M. Criado-Sancho, *Thermodynamics of Fluids under Flow*, 2nd edition, Springer, Dordrecht, Heidelberg, London, New York, 2011.

40. C. Cattaneo, Sulla conduzione del calore, *Atti Seminario Mat. Fis. Univ. Modena* 3 (1948) 83-101.

41. W. Dreyer and H. Struchtrup, Heat pulse experiments revisited, *Continuum Mech. Thermodyn*. 5 (1993) 3-50.

42. S. Hess, On nonlocal constitutive relations, continued fraction expansion for the wave vector dependent diffusion coefficient, *Z. Naturforsch*. 32a (1977) 678-684.

43. D. Jou, J. Casas-Vazquez, G. Lebon, M. Grmela, A phenomenological scaling approach for heat transport in nano-systems, *Appl. Math. Lett.* 18 (2005) 963-967.

Figure captions

Figure 1. Effective heat conductivity of Si-Ge nanocomposite versus the volume fraction of Si nanoparticle at room temperature for different radii r_p = *5 nm(*a), *25 nm* (b), *100 nm* (c) and different *s* values (*s=0, 0.2, 1*).

Figure 2. Effective heat conductivity of SiO_2 embedded in an epoxy resin versus the volume fraction and comparison with experimental data at room temperature (r_p=10 nm, *s*=0). General trend in the region $0<\varphi<1$ (a). Zoom on the region $0< \varphi <0.10$ (b).

Figure 3. Effective heat conductivity of Si-Ge nanocomposite versus the volume fraction at three different temperature: *T=200K* (upper curves), *T= 300K* (middle curves), *T= 500K*

(bottom curves), different radii r_p = *5*, *25*, *100 nm* and different *s* values *s=0* (a), *s= 0.2* (b), *s=0.5* (c).

Figure 4. Effective thermal conductivity of Si-Ge versus the temperature at three different values of the volume fraction: φ*=0.01*(a), φ*=0.2*(b), φ*=0.5*(c) for r_p*=5, 25, 100 nm*, with *s* = 0. For the sake of comparison, the values λ_m for pure Ge are also plotted.

Table caption

Table 1. Material parameters (at room temperature)